J Porous Mater (2016) 23:823–831
DOI 10.1007/s10934-016-0137-8

Structure and catalytic oxidative desulfurization properties of SBA-15 supported silicotungstic acid ionic liquid

Junjie Yuan[1] · Jun Xiong[2] · Jiahong Wang[2] · Wenjing Ding[2] · Lei Yang[2] · Ming Zhang[3] · Wenshuai Zhu[2] · Huaming Li[3]

Published online: 6 February 2016
© Springer Science+Business Media New York 2016

Abstract A supported catalyst was synthesized on the mesoporous materials with ionic liquid modified by the silicontungstic acid (HSiW-IL/SBA-15). A series of characterization, such as XRD, N_2 adsorption desorption, SEM, TEM and XPS analysis showed that HSiW was successfully immobilized onto the IL modified SBA-15 and maintained the SBA-15 mesoporous structure. Compared with HSiW and HSiW/SBA-15, the catalyst HSiW-IL/SBA-15 had excellent catalytic activity for oxidative desulfurization of fuels. After analysis, the high activity of HSiW-IL/SBA-15 was attributed to the catalyst with large specific surface area, pore size and hydrophobic performance, which had a better wettability for fuel. The catalyst had a good recycling performance, and the sulfur removal still remained 96.4 % after eight times cycle.

Keywords Supported catalyst · Silicontungstic acid · Ionic liquid · Oxidative desulfurization · Wettability

Electronic supplementary material The online version of this article (doi:10.1007/s10934-016-0137-8) contains supplementary material, which is available to authorized users.

✉ Wenshuai Zhu
zhuws@ujs.edu.cn

✉ Huaming Li
lihm@ujs.edu.cn

[1] School of Agricultural Equipment Engineering, Institute of Agricultural Engineering, Jiangsu University, Zhenjiang 212013, China

[2] School of Chemistry and Chemical Engineering, Jiangsu University, Zhenjiang 212013, China

[3] Institute for Energy Research, Jiangsu University, Zhenjiang 212013, China

1 Introduction

The SO_x is produced by the combustion of fossil fuels, especially diesel oils, which leads to acid rain and damages exhaust after-treatment devices [1–4]. As a consequence, it becomes the most urgent task to achieve deep desulfurization in the industrial process. At present, catalytic hydrodesulfurization (HDS), as a traditional desulfurization method, has been used for industrial application. This method can effectively remove mercaptans, sulfide and disulfide removal, but for thiophene-type sulfide, such as dibenzothiophene (DBT) and its derivatives, the reaction conditions of HDS is harsh [5–7]. In this case, it is very necessary to achieve deep desulfurization method without high temperature, high pressure and hydrogen [8]. In this regard, many research groups reported that deep oxidative desulfurization (ODS) is considered to be one of the promising desulfurization technologies under mild condition, without hydrogen participates [9–17]. The technology is the oxidation of organic sulfides to the corresponding sulfoxide and sulfone, followed by extraction or adsorption to achieve deep desulfurization of fuels.

In organic oxidation reaction, hydrogen peroxide (H_2O_2) is widely regarded as a kind of green and efficient oxidant [18–21]. Therefore, a series of catalysts were designed, such as Au [22], silica sulfuric acid [23], TiO_2 nanocrystalline [24], tantalum chloride [25] and Si–V [26] etc. It is worth noting that the catalyst containing Mo or W has a good catalytic activity in the oxidative desulfurization system, such as MoO_2Cl_2 [27], $PPh_4[MO(O_2)_2L]$ (M = Mo or W) [28], WO_3/MCM-48 [29], $Na_2WO_4/C_6H_5PO_3H_2/[CH_3(n\text{-}C_8H_{17})_3N]HSO_4$ [30], WO_4^{2-}/silica-NH_3^+ [31] and so on. Polyoxometalates (POMs) are a class of well-defined transition metal oxygen clusters with adjustable properties such as redox and acid, and used as catalysts for various organic transformation [32], which have been previously reported in the literature and on

polyoxophosphomolybdate and polyoxophosphotungstate as catalysts, H_2O_2 as oxidant in the desulfurization system [33]. However, these catalysts usually formed homogeneous or two-phase system, which led to the difficulty of separating the catalyst from the recovery [34]. In order to solve this problem, many strategies were developed to make POMs supported on the porous materials. However, other problems are still not solved, such as slow reaction rate, loss of active components and complicated synthesis step of the catalyst. Ionic liquids (ILs) are often used as a reaction medium and catalyst [35–37], which can combined with POM anion and exhibited high redox properties and catalytic activity [38, 39].

In this study, a chemical bond strategy, $H_4[SiO_4(W_3O_9)_4]$ was supported on ionic liquid modified SBA-15 (denoted as HSiW-IL/SBA-15). HSiW-IL/SBA-15 as the catalyst and H_2O_2 as the oxidant, the oxidative desulfurization performance was investigated. As a catalyst, HSiW-IL/SBA-15 shows high desulfurization efficiency and good recycling performance under mild reaction conditions.

2 Experimental section

2.1 Materials

All the chemicals used in the study were analytical purity and were used as received. Sulfide and poly(ethylene glycol)-block-poly(propylene glycol)-block-poly(ethylene glycol) (Pluronic P123) were purchased from Sigma-Aldrich. Commercially available 30 wt% H_2O_2, $H_4[SiO_4(W_3O_9)_4]$ (HSiW), n-octane, tetrade-cane, ethylsilicate (TEOS), and N-methylimidazole were purchased from Sinopharm Chemical Reagent. (3-chloropropyl)Trimethoxysilan (98 %) was marketed by Aladdin Chemistry.

2.2 Preparation of catalysts

1-methyl-3-(trimethoxysilylpropyl)-imidazolium chloride ([pmim]Cl), SBA-15 and [pmim]Cl-SBA-15, denoted as IL/SBA-15 were prepared according to the procedures reported previously [39]. The catalysts of xHSiW-IL/SBA-15 with different loadings of HSiW on IL/SBA-15 were synthesized by adding 0.5 g IL/SBA-15 into 50 mL HSiW aqueous solution and stirring at room temperature for 12 h, where x represents the weight of HSiW in the samples. Then, the obtained samples were isolated by filtration and washed with deionized water. The resulting solid was dried in vacuum at 50 °C for 24 h. The weight contents of HSiW were 0.05, 0.1, 0.2 and 0.3 g (Scheme 1).

HSiW/SBA-15 was prepared similar to the aforementioned method. 0.5 g SBA-15 was added into 50 mL of deionized water containing 0.05 g silicotungstic acid, and the mixture was stirred at room temperature for 12 h. Then, the solid was isolated by filtration and washed with deionized water. The resulting solid was dried in vacuum at 50 °C for 24 h to produce HSiW/SBA-15.

2.3 Characterization of catalysts

Powder X-ray diffraction (XRD) analysis was carried out on Bruker D8 diffractometer with high-intensity Cu Kα ($\lambda = 1.54$ A). X-ray photoemission spectroscopy (XPS) was recorded on a VG Mul-tiLab 2000 system with a monochromatic Mg–K a source operated at 20 kV. The morphological structures of catalysts measurements were carried out with a field-emission scanning electron microscope (SEM) (JEOL JSM-7001F) equipped with an energy-dispersive X-ray spectroscope (EDS) operated at an acceleration voltage of 10 kV. Transmission electron microscopy (TEM) micrographs were taken with a JEOL-JEM-2010 (JEOL, Japan) operating at 200 kV. The samples used for TEM were prepared by dispersing a small amount of the product in ethanol, placing a drop of the solution onto a copper grid, and letting the ethanol evaporate slowly in the air. The N_2 adsorption–desorption isotherms at 77 K were investigated using a TriStar II 3020 surface area and porosity analyzer (Micromeritics Instrument).

2.4 Preparation of model oil and desulfurization procedure

Model oil was prepared by dissolving DBT, benzothiophene (BT), and 4,6-dimethyldibenzothiophene (4,6-DMDBT) in n-octane with their initial S-content of 500, 500, and 232 ppm, respectively. In a typical desulfurization experiment, 0.01 g catalyst and 5 mL model oil were added to a 40 mL two-necked flask. Then 30 wt% hydrogen peroxide was added within 10 min with magnetic stirring at the corresponding temperature. After the reaction, the concentration of sulfur-containing compounds in the model oil were analyzed by a Gas Chromatography-Flame Ionization Detector (GC-FID) with tetradecane as the internal standard (Agilent 7890A; HP-5, 30 m × 0.32 mm i.d. × 0.25 μm; FID: Agilent). Gas Chromatography–Mass Spectrometer (GC–MS) (Agilent 7890/5975C-Gas Chromatography (GC)/Mass Selective Detector (MSD); HP-5 MS column, 30 m × 250 mm i.d. × 0.25 mm; temperature program: 100 °C temperature rising 15 °C min^{-1} until 200 °C for 10 min) was also used to analyze the oxidized S-compounds after reaction.

3 Results and discussion

3.1 Characterization of the catalyst

The low-angle XRD patterns of the SBA-15, IL/SBA-15 and the functionalized HSiW-IL/SBA-15 catalysts are

Scheme 1 The synthetic process of HSiW-IL/SBA-15

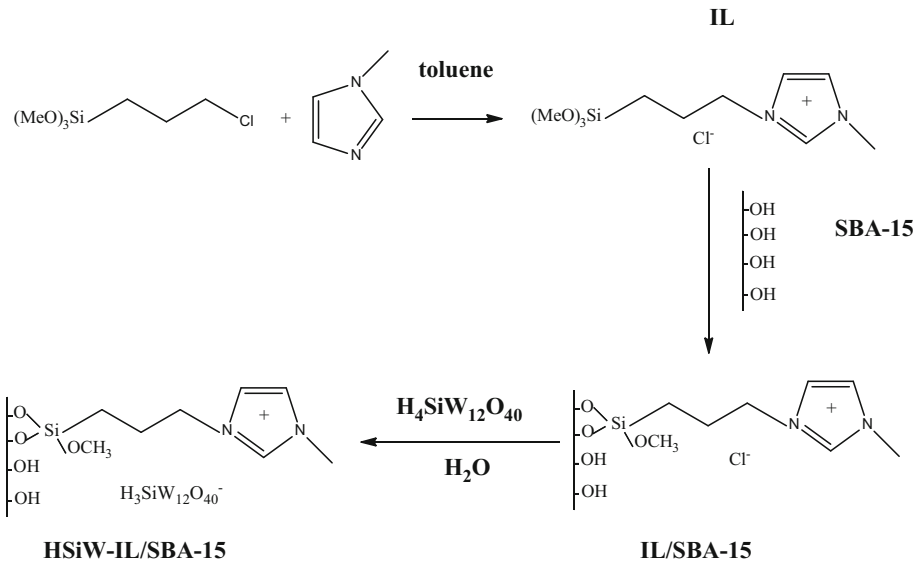

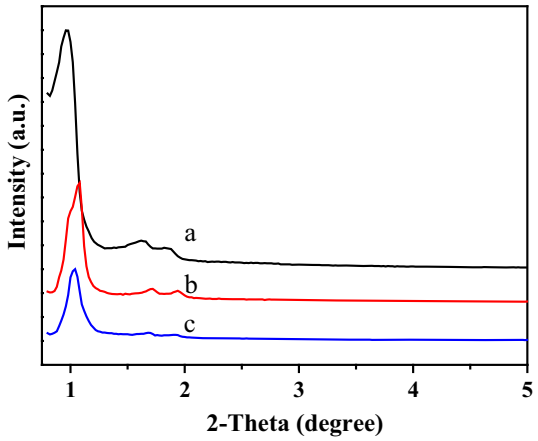

Fig. 1 The low-angle XRD of SBA-15 (*a*), IL/SBA-15 (*b*) and 0.2HSiW-IL/SBA-15 (*c*)

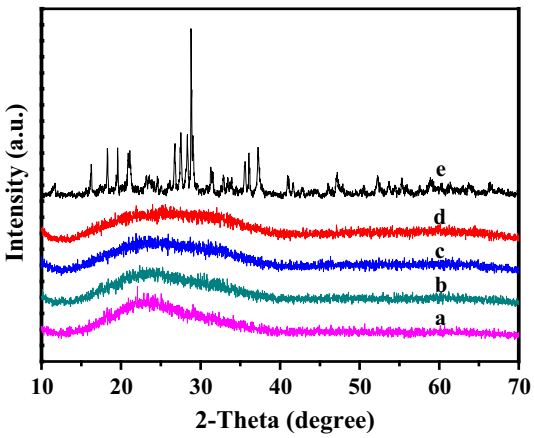

Fig. 2 The wide-angle XRD of HSiW and different HSiW loading amount samples. (*a*) 0.05HSiW-IL/SBA-15, (*b*) 0.1HSiW-IL/SBA-15, (*c*) 0.2HSiW-IL/SBA-15, (*d*) 0.3HSiW-IL/SBA-15, (*e*) HSiW

presented in Fig. 1. It is clearly shown that SBA-15 is consisted of one very intense diffraction peak ($2\theta \approx 1.0°$) for d_{100} and two less intense diffraction peaks ($2\theta = 1–2°$) for d_{110} and d_{200}. Precursor IL/SBA-15 showed three weaker peaks. And all peaks showed a shift to large angles, which illustrated that the IL was supported on SBA-15 [38–40]. Compared with IL/SBA-15, the diffraction peak intensity of the catalyst HSiW-IL/SBA-15 further decreased, but the peaks still could be observed. The results indicated that the HSiW was successfully supported on IL/SBA-15 and the structure ordering of SBA-15 was maintained after the HSiW incorporated.

Low-angle XRD patterns of the catalysts with different HSiW loadings were shown in Fig. 1S. It can be seen that the increase of the loading amount, the intensity of the (100), (110) and (200) three peaks were gradually decrease. When the loading amount increased to 0.3 g, the (110) and (200) peaks almost disappeared. As the increase of the HSiW loading, the SBA-15 would be blocked, resulting in the little decrease of the mesoporous degree of the order.

The wide-angle XRD pattern of HSiW and the HSiW-IL/SBA-15 with different HSiW loading (0.05–0.3 g) is shown in Fig. 2. There was no obvious peak of HSiW in all catalysts, which may be due to the low loading amount of HSiW or a high dispersion of HSiW on the carrier [41]. The wide angle peak at $2\theta = 23°$ merged into a broad amorphous silica peak. It can be seen that an increase in loading of the amount, the peak became wider and the intensity was smaller, suggesting that the introduction of HSiW can affect the structure of SBA-15.

The FTIR spectra of HSiW and HSiW-IL/SBA-15 are depicted in Fig. 3. The absorption bands at 979, 924, and 793 cm^{-1} were ascribed to HSiW [42, 43]. It can be observed these characteristic bands of HSiW could be

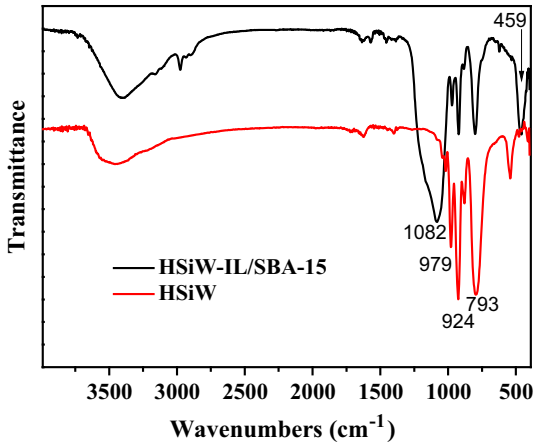

Fig. 3 The FTIR spectra of HSiW and HSiW-IL/SBA-15

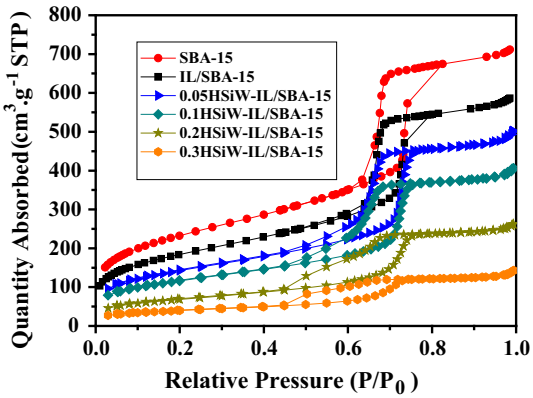

Fig. 4 N_2 adsorption–desorption isotherms of the samples

found in HSiW-IL/SBA-15. For HSiW-IL/SBA-15, the absorption bands at 1082 and 459 cm^{-1} are attributed to the asymmetric and symmetric stretch of Si–O–Si, respectively [39, 44], which is the skeleton of SBA-15. Besides, C–H vibrations peaks of ionic liquid at about 2975 cm^{-1} could also be seen. Thus, it can conclude that HSiW and IL were successfully supported on SBA-15.

The nitrogen adsorption–desorption isotherms for SBA-15, IL/SBA-15, and HSiW-IL/SBA-15 catalysts were shown in Fig. 4. It can be observed that SBA-15 was a typical IV type adsorption–desorption isotherm, with the H1 type hysteresis loop, which showed that the synthesized SBA-15 had a regular circular hole. Compared with SBA-15, 0.05HSiW-IL/SBA-15 and IL/SBA-15 also were IV type adsorption adsorption–desorption isotherms with hysteresis loops for H1 type, however it can clearly see that the decreasing the adsorption capacity of the three samples illustrated decreasing of the specific surface area. The result implied that HSiW was successfully loaded onto ionic liquid modified SBA-15, which was consistent with the low-angle XRD. With regard to catalysts with different HSiW loadings, with the increase of HSiW loading, although the sample retained IV type adsorption isotherm, the hysteresis loop had changed, and the adsorption capacity decreased with the increase of the loading amount. It was found that the samples with different HSiW loading capacity maintained the mesoporous structure, but the increase of HSiW loading led to the specific surface area decreasing. This was consistent with the results of Fig. S1. Table 1 is the structure properties of the samples, which was based on the N_2 adsorption desorption analysis.

The SEM images in Fig. 5 show the variation in morphology of the SBA-15 and the catalyst HSiW-IL/SBA-15. As can be seen from the images, the morphology of the catalyst HSiW-IL/SBA-15 was the same with the carrier SBA-15, which further showed that the HSiW ionic liquid modified SBA-15 did not change the morphology of the carrier SBA-15. Figure 5c is the EDS analysis of the catalyst HSiW-IL/SBA-15. It can be seen, the catalyst was composed of C, O, Si, N and W elements. All the elements of the ionic liquid and the HSiW can be found, and this further illustrated that the HSiW had been successfully loaded onto the IL modified SBA-15. The morphology of the sample can be directly reflected by the transmission electron microscope (TEM). Figure 6 shows TEM micrographs of SBA-15 and 0.2HSiW-IL/SBA-15 sample. It showed that SBA-15 displayed highly ordered mesopore channels, and after HSiW-IL was anchored on SBA-15, the catalyst still maintained ordered structure.

XPS spectra were used to analyze the surface chemical composition of 0.2HSiW-IL/SBA-15. Figure 7 is the total XPS spectrum of 0.2HSiW-IL/SBA-15. It can be seen that the catalyst is composed of N, O, Si, P, W and C. Elements N, O, C were derived from the ionic liquid. The binding

Table 1 The structure properties of the samples

Sample	S_{BET} (m^2 g^{-1})	Pore volume (cm^3 g^{-1})	Pore size (nm)
SBA-15	842	1.01	5.9
IL/SBA-15	666	0.92	5.6
0.05HSiW-IL/SBA-15	511	0.80	5.6
0.1HSiW-IL/SBA-15	416	0.65	5.4
0.2HSiW-IL/SBA-15	204	0.40	5.0
0.3HSiW-IL/SBA-15	141	0.23	5.0

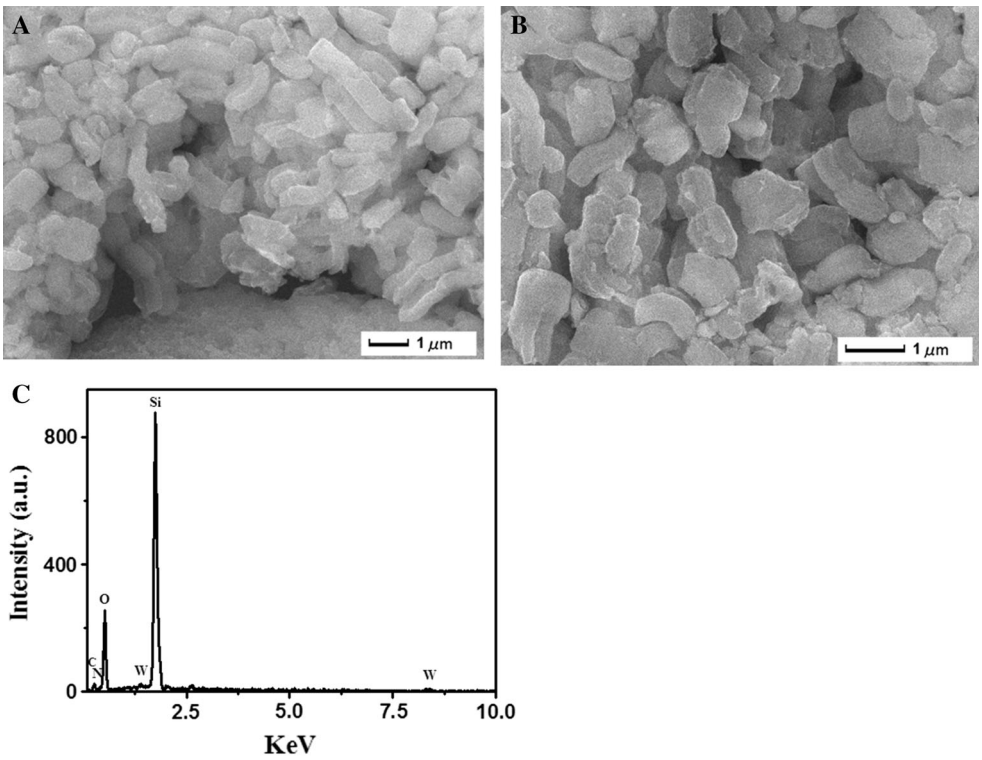

Fig. 5 SEM images of **a** SBA-15, **b** 0.2HSiW-IL/SBA-15 and **c** EDS of the 0.2HSiW-IL/SBA-15

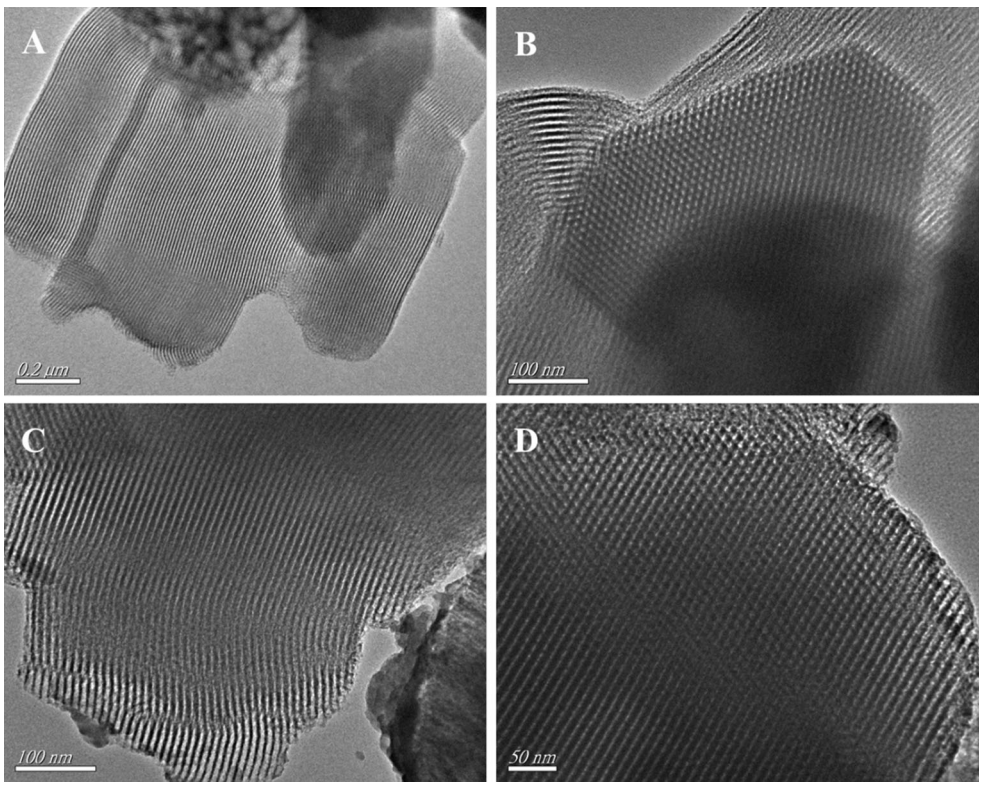

Fig. 6 TEM images of SBA-15 (**a**, **b**) and 0.2HSiW-IL/SBA-15 (**c**, **d**)

energies obtained in the XPS analysis are corrected for specimen charging by internally referring to the adventitious carbon at a binding energy of 284.6 eV. From the high resolution spectrum (Fig. 7f), it can be seen that there were two peaks assigning to W4f in 35.6 and 37.6 eV, which indicated that the HSiW was also successfully introduced.

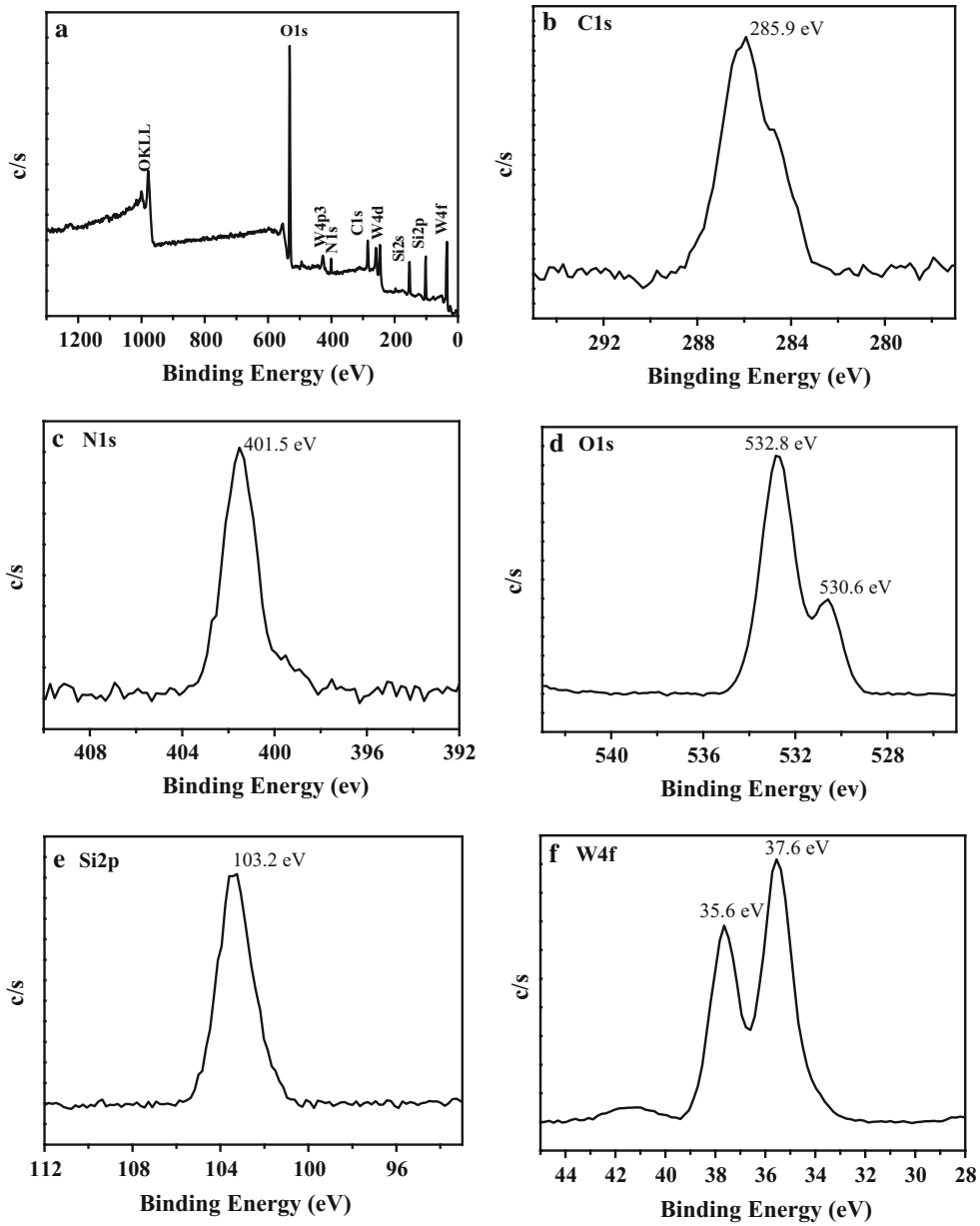

Fig. 7 XPS spectra of 0.2HSiW-IL/SBA-15. **a** Survey of the sample, **b** C1s, **c** N1s, **d** O1s, **e** Si2p, **f** W4f

The above results are in good agreement with the literature [45, 46]. Moreover, the XPS tests of HSiW and IL/SBA-15 have been performed to verify the interaction of IL or HSiW and the support SBA-15. From the Fig. 8, it can be seen that with regard to HSiW-IL/SBA-15, the binding energy of W4f, W4d, and Si2d shifted towards low value, compared with that of HSiW and IL/SBA-15. The result further verified the interaction between HSiW and IL/SBA-15.

3.2 Effect of different catalysts on the removal of DBT

The effect of HSiW, 0.2HSiW/SBA-15 and 0.2HSiW-IL/SBA-15 three catalysts on the removal of DBT were investigated. As shown in Fig. 9, the HSiW and 0.2HSiW/SBA-15 had little catalytic activity on the removal of DBT. Under the same experimental conditions, as for the 0.2HSiW-IL/SBA-15 catalyst, the removal rate of DBT could reach 97.9 %. It indicated that the IL has a very important effect on the desulfurization reaction. In order to study the reason, the contact angle measurements of HSiW/SBA-15 and HSiW-IL/SBA-15 were carried out. As can be seen from Fig. 10, when a water droplet was dropped to contact the surface of HSiW/SBA-15, the contact angle was zero. However, the contact angle was 50° for a water droplet in contact with the surface of HSiW-IL/SBA-15. It is shown that there are some hydrophobic properties of the IL modified catalyst. It is understood that the hydrophobic

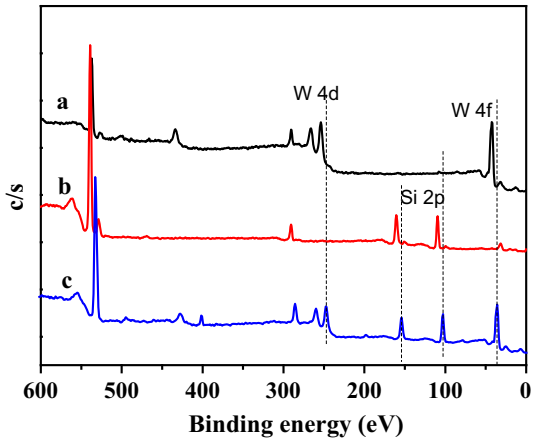

Fig. 8 XPS spectra of (*a*) HSiW, (*b*) IL/SBA-15 and (*c*) HSiW-IL/SBA-15

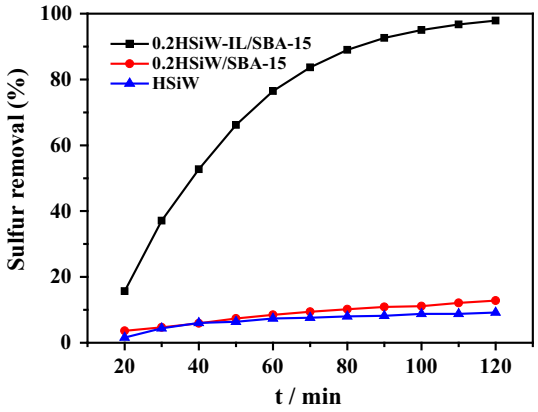

Fig. 9 Oxidative removal of DBT on different catalysts HSiW, 0.2HSiW/SBA-15 and 0.2HSiW-IL/SBA-15

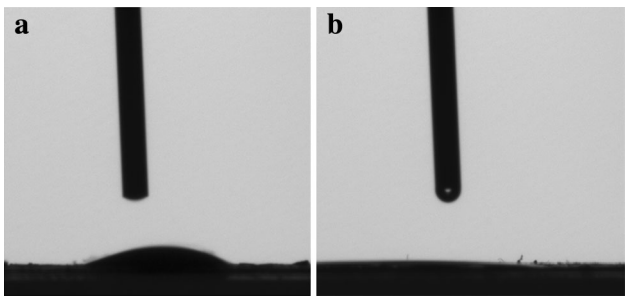

Fig. 10 Contact angle for a water droplet on the surface of HSiW-IL/SBA-15 (**a**) and HSiW/SBA-15 (**b**)

material has a good wettability for the model oil. This shows that with the hydrophobic catalyst HSiW-IL/SBA-15 can expose more active sites in the model oil. Therefore, the HSiW-IL/SBA-15 exhibited higher catalytic activity to remove the DBT from the model oil and had a great relationship with the good wettability of the reactants.

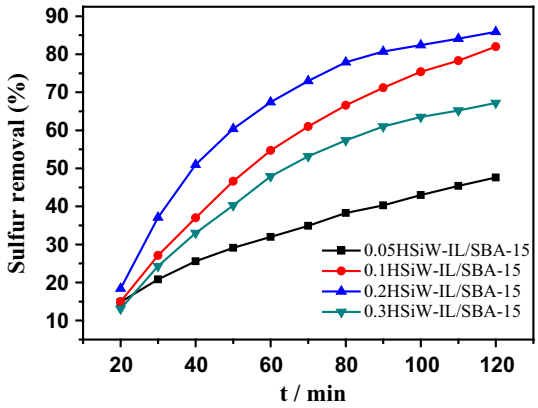

Fig. 11 Oxidative removal of DBT of different HSiW loadings. Experimental conditions: 5 mL model oil, m (catalyst) = 0.02 g, n (H_2O_2)/n(S) = 3:1, T = 60 °C

3.3 Effect of different HSiW loading on removal of DBT

Figure 11 shows the effect of different HSiW supported catalysts of 0.05HSiW-IL/SBA-15, 0.1HSiW-IL/SBA-15, 0.2HSiW-IL/SBA-15, and 0.3HSiW-IL/SBA-15 on the removal of DBT. When the HSiW increased from 0.05 to 0.2 g, the removal of DBT was 47.6, 82.0, and 85.9 %, respectively. When the loading amount of HSiW further increased to 0.3, the desulfurization activity was reduced to 67.2 %. This was because over much loading amount of HSiW blocked the pore channel of SBA-15. Also, the surface area and pore size became smaller, which influenced the mass transfer, and is not conducive to the desulfurization reaction. The removal effect of DBT on 0.2HSiW-IL/SBA-15 was the best, so 0.2HSiW-IL/SBA-15 was chosen in the following investigation.

3.4 Optimization of reaction parameters

3.4.1 Influence of the time and temperature on sulfur removal

The effect of different time and reaction temperature on the removal of DBT was studied in Fig. 12. As can be seen, with the increase of temperature, the reaction rate increased, and the DBT removal of model oil increased. When the reaction temperature was 40 °C within 120 min, the sulfur removal is only 20.9 %. When the reaction temperature increased to 50 °C, the sulfur removal increased to 76.1 %, and the sulfur removal reached 97.9 % when the reaction temperature was 60 °C. Continuously increase reaction temperature, the sulfur removal could rise. However, when the reaction temperature was 60 °C within 120 min, the deep desulfurization could achieve. Considering the economic and industrial application, the lower temperature (60 °C) was chosen as a good reaction temperature.

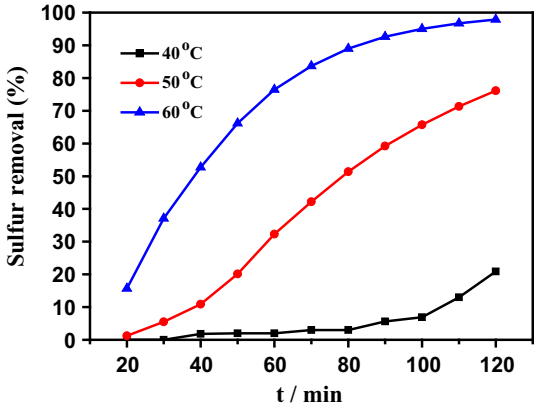

Fig. 12 Effect of different reaction temperature and time on DBT removal. Experimental conditions: 5 mL model oil, m (catalyst) = 0.02 g, n (H_2O_2)/n(S) = 4:1

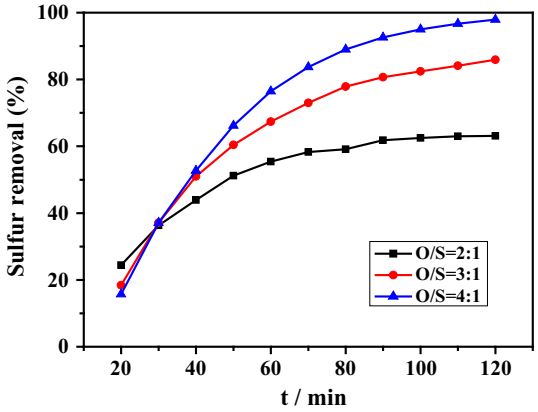

Fig. 13 Effect of different amount of H_2O_2 on DBT removal. Experimental conditions: 5 mL model oil, m (catalyst) = 0.02 g, T = 60 °C

3.4.2 Effect of the amount of H_2O_2 on the sulfur removal

As shown in Fig. 13, the desulfurization effect of different H_2O_2/S molar ratio was investigated. Based on the stoichiometric ratio, 1 mol DBT was oxidized into $DBTO_2$ need to consume 2 mol H_2O_2. When the H_2O_2/S molar ratio was 2:1, the sulfur removal was only 63.1 %. This was because hydrogen peroxide involved two reactions in the process: oxidation of sulfur compounds in the oil and its own decomposition reaction [47]. The sulfur removal was 85.9 % of O/S = 3:1 at 120 min. When the H_2O_2/S molar ratio increased to 4:1, the sulfur removal could reach 97.9 %, which met the purpose of deep desulfurization.

3.5 Investigation of oxidizing products

In order to investigate the oxidizing products of sulfide, DBT was selected as the object of study. After the oxidation reaction, the model oil was analyzed by GC–MS. As can be seen in Fig. 14, the DBT oxidizing products $DBTO_2$ was also detected in the model oil, suggesting that when 0.2HSiW-IL/SBA-15 as catalyst, H_2O_2 as oxidant, DBT was oxidized to DBT sulfone.

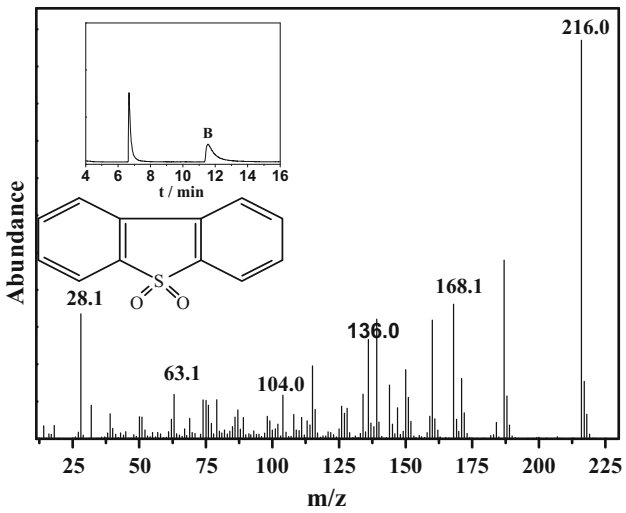

Fig. 14 Mass spectrogram of oil phase after the reaction

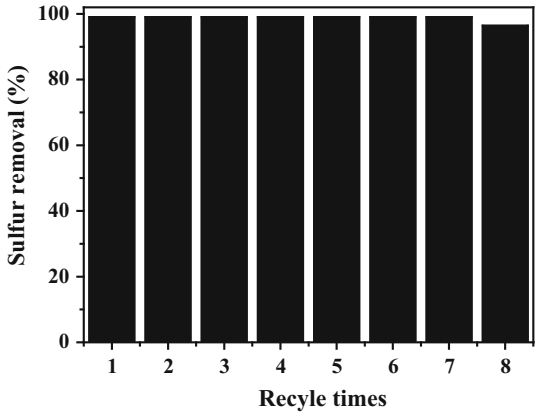

Fig. 15 Recycle of the reaction system. Experimental conditions: 5 mL model oil, m (catalyst) = 0.02 g, n (H_2O_2)/n(S) = 4:1, t = 120 min, T = 60 °C

3.6 Recyclability

Figure 15 shows the recycle effect of the reaction system on the removal of DBT in model oil. After the end of the reaction system, the catalyst precipitation on the lower level, the reaction of oil can be simply directly through the pouring process separated from the system, and then added the new model oil and H_2O_2 for the next reaction system. Through the graph, we can see that the system can recycle eight times for the desulfurization with a little decrease.

4 Conclusion

In summary, we introduced ionic liquid modified on SBA-15, and a series of characterization results demonstrated that the HSiW is successfully loaded onto the ionic liquid modified SBA-15, and the supported catalyst keeps the mesoporous structure of SBA-15. These results seem to be related to better wettability on the catalyst HSiW-IL/SBA-15 for model oil. In the experimental system, the effects of different HSiW loading, reaction temperature and hydrogen peroxide dosage on the DBT desulfurization rate were investigated, and the optimum reaction conditions were determined. The detection for the major oxidizing product is sulfone, and after recycling 8 times, the supported catalyst still exhibits high stability and catalytic activity, the sulfur removal is obtained 96.4 %.

Acknowledgments We thank the National Nature Science Foundation of China (Nos. 21276117, 21576122, 21406092), Six Big Talent Peak in Jiangsu province (JNHB-004), Postdoctoral Foundation of China (No. 2014M551516).

References

1. J. Xiao, L.M. Wu, Y. Wu, B. Liu, L. Dai, Z. Li, Q.B. Xia, H.X. Xi, Appl. Energy **113**, 78 (2014)
2. W.S. Zhu, C. Wang, H.P. Li, P.W. Wu, S.H. Xun, W. Jiang, Z.G. Chen, Z. Zhao, H.M. Li, Green Chem. **17**, 2464 (2015)
3. H.Y. Lü, J.B. Gao, Z.X. Jiang, Y.X. Yang, B. Song, C. Li, Chem. Commun. **150** (2007)
4. H.P. Li, Y.H. Chang, W.S. Zhu, W. Jiang, M. Zhang, J.X. Xia, S. Yin, H.M. Li, J. Phys. Chem. B **119**, 5995 (2015)
5. F.T. Li, B. Wu, R.H. Liu, X.J. Wang, L.J. Chen, D.S. Zhao, Chem. Eng. J. **274**, 192 (2015)
6. J. Xiong, W.S. Zhu, H.P. Li, W.J. Ding, Y.H. Chao, P.W. Wu, S.H. Xun, M. Zhang, H.M. Li, Green Chem. **17**, 1647 (2015)
7. J. Xiong, W.S. Zhu, H.P. Li, L. Yang, Y.H. Chao, P.W. Wu, S.H. Xun, W. Jiang, M. Zhang, H.M. Li, J. Mater. Chem. A **3**, 12738 (2015)
8. W. Jiang, W.S. Zhu, H.P. Li, X. Wang, S. Yin, Y.H. Chang, H.M. Li, Fuel **140**, 590 (2015)
9. W.H. Wang, G. Li, W.G. Li, L.P. Liu, Chem. Commun. **47**, 3529 (2011)
10. W.S. Zhu, B.L. Dai, P.W. Wu, Y.H. Chao, J. Xiong, S.H. Xun, H.P. Li, H.M. Li, ACS Sustain. Chem. Eng. **3**, 186 (2015)
11. P.W. Wu, W.S. Zhu, Y.H. Chao, J.S. Zhang, P.F. Zhang, H.Y. Zhu, C.F. Li, Z.G. Chen, H.M. Li, S. Dai, Chem. Commun. **52**, 144 (2016)
12. X.M. Zhou, W. Chen, Y.F. Song, Eur. J. Inorg. Chem. **2014**, 812 (2014)
13. M. Chamack, A.R. Mahjoub, H. Aghayan, Chem. Eng. J. **255**, 686 (2014)
14. W.S. Zhu, P.W. Wu, L. Yang, Y.H. Chang, Y.H. Chao, H.M. Li, Y.Q. Jiang, W. Jiang, S.H. Xun, Chem. Eng. J. **229**, 250 (2013)
15. W. Zhang, H. Zhang, J. Xiao, Z.X. Zhao, M.X. Yu, Z. Li, Green Chem. **16**, 211 (2014)
16. H.Y. Song, J.J. Gao, X.Y. Chen, J. He, C.X. Li, Appl. Catal. A **456**, 67 (2013)
17. B.S. Li, Z.X. Liu, J.J. Liu, Z.Y. Zhou, X.H. Gao, X.M. Pang, H.T. Sheng, J. Colloid Interface Sci. **362**, 450 (2011)
18. X. Jiang, H.M. Li, W.S. Zhu, L.N. He, H.M. Shu, J.D. Lu, Fuel **88**, 431 (2009)
19. J. Zhang, A.J. Wang, Y.J. Wang, H.Y. Wang, J.Z. Gui, Chem. Eng. J. **245**, 65 (2014)
20. P.W. Wu, W.S. Zhu, A.M. Wei, B.L. Dai, Y.H. Chao, C.F. Li, H.M. Li, S. Dai, Chem. Eur. J. **21**, 15421 (2015)
21. J. Zhang, A.J. Wang, X. Li, X.H. Ma, J. Catal. **279**, 269 (2011)
22. Y. Yuan, Y.B. Bian, Tetrahedron Lett. **48**, 8518 (2007)
23. A. Shaabani, A.H. Rezayan, Catal. Commun. **8**, 1112 (2007)
24. A. Al-Maksoud, S. Daniele, A.B. Sorokin, Green Chem. **10**, 447 (2008)
25. M. Kirihara, J. Yamamoto, T. Noguchi, Y. Hirai, Tetrahedron Lett. **50**, 1180 (2009)
26. F. Gregori, I. Nobili, F. Bigi, R. Maggi, G. Predieri, G.J. Sartori, Mol. Catal. A Chem. **286**, 124 (2008)
27. K. Jeyakumar, D.K. Chand, Tetrahedron Lett. **47**, 4573 (2006)
28. N. Gharah, S. Chakraborty, A.K. Mukherjee, R. Bhattacharyya, Inorg. Chim. Acta **362**, 1089 (2009)
29. D.H. Koo, M. Kim, S. Chang, Org. Lett. **7**, 5015 (2005)
30. K. Sato, M. Hyodo, M. Aoki, X.Q. Zheng, R. Noyori, Tetrahedron **57**, 2469 (2001)
31. B. Karimi, M. Ghoreishi-Nezhad, J.H. Clark, Org. Lett. **7**, 625 (2005)
32. M. Misono, Chem. Commun. **13**, 1141 (2001)
33. W.S. Zhu, H.M. Li, X. Jiang, Y.S. Yan, J.D. Lu, J.X. Xia, Energy Fuels **21**, 2514 (2007)
34. X.Y. Shi, J.F. Wei, J. Mol. Catal. A: Chem. **280**, 142 (2008)
35. T.L. Greaves, C.J. Drummond, Chem. Rev. **108**, 206 (2008)
36. W.L. Huang, W.S. Zhu, H.M. Li, H. Shi, G.P. Zhu, H. Liu, G.Y. Chen, Ind. Eng. Chem. Res. **49**, 8998 (2010)
37. W.S. Zhu, G.P. Zhu, H.M. Li, Y.H. Chao, Y.H. Chang, G.Y. Chen, C.R. Han, J. Mol. Catal. A: Chem. **347**, 8 (2011)
38. J. Xiong, W.S. Zhu, W.J. Ding, L. Yang, Y.H. Chao, H.P. Li, F.X. Zhu, H.M. Li, Ind. Eng. Chem. Res. **53**, 19895 (2014)
39. J. Xiong, W.S. Zhu, W.J. Ding, L. Yang, M. Zhang, W. Jiang, Z. Zhao, H.M. Li, RSC Adv. **5**, 16847 (2015)
40. X.M. Yan, P. Mei, J.H. Lei, Y.Z. Mi, L. Xiong, L.P. Guo, J. Mol. Catal. A: Chem. **304**, 52 (2009)
41. X.M. Yan, P. Mei, L. Xiong, L. Gao, Q.F. Yang, L.J. Gong, Catal. Sci. Technol. **3**, 1985 (2013)
42. M. Klein, A. Varvak, E. Segal, B. Markovsky, I.N. Pulidindi, N. Perkas, A. Gedanken, Green Chem. **17**, 2418 (2015)
43. J. Chen, X.L. Fang, X.P. Duan, L.M. Ye, H.Q. Lin, Y.Z. Yuan, Green Chem. **16**, 294 (2014)
44. X.C. Shao, X.T. Zhang, W.G. Yu, Y.Y. Wu, Y.C. Qin, Z.L. Sun, L.J. Song, Appl. Surf. Sci. **263**, 1 (2012)
45. S. Echeandiaa, P.L. Ariasa, V.L. Barrioa, B. Pawelecb, J.L.G. Fierro, Appl. Catal. B Environ. **101**, 1 (2010)
46. R.M. Ladera, M. Ojeda, J.L.G. Fierro, S. Rojas, Catal. Sci. Technol. **5**, 484 (2015)
47. J. Xiong, W.S. Zhu, H.M. Li, Y.H. Xu, W. Jiang, S.H. Xun, H. Liu, Z. Zhao, AIChE J. **59**, 4696 (2013)